The first observation of dynamical chirality by means of polarized neutron scattering in the triangular-lattice antiferromagnet $CsMnBr_3$

1998 J. Phys.: Condens. Matter 10 951

(http://iopscience.iop.org/0953-8984/10/5/005)

J. Phys.: Condens. Matter **10** (1998) 951–960. Printed in the UK PII: S0953-8984(98)86141-9

The first observation of dynamical chirality by means of polarized neutron scattering in the triangular-lattice antiferromagnet $CsMnBr_3$

S V Maleyev†, V P Plakhty†, O P Smirnov†, J Wosnitza‡, D Visser§, R K Kremer‖ and J Kulda¶

† Petersburg Nuclear Physics Institute, Gatchina, St Petersburg, 188350, Russia
‡ Physikalisches Institut, Universität Karlsruhe, 76128 Karlsruhe, Germany
§ Department of Physics, University of Warwick, Coventry CV4 7AL, UK
‖ Max-Planck-Institut Stuttgart, 70506 Stuttgart, Germany
¶ Institut Laue–Langevin, BP 156, 38042 Grenoble Cédex 9, France

Received 15 July 1997, in final form 27 October 1997

Abstract. The polarization-dependent part of the neutron scattering in the triangular-lattice antiferromagnet $CsMnBr_3$ is studied. This scattering appears in an external magnetic field and is determined by the projection of a chiral fluctuation on the sample magnetization (the dynamical chirality, DC). It is shown that the DC cross section is an odd function of the energy transfer, ω, and is proportional to the magnetic field up to 10 kOe above T_N. A Be filter is used instead of the analyser for measuring the DC scattering integrated over $\omega < 0$. It is shown that below T_N the field dependence of this intensity reveals two features related to the acoustic spin waves and to a new type of low-energy magnetic excitation, presumably of topological nature. The temperature dependence of the acoustic spin waves near T_N is in qualitative agreement with dynamical scaling.

The frustrated triangular-lattice antiferromagnets (TLA) are currently being intensively studied. The main interest arises from Kawamura's idea [1] that magnetic phase transitions in such compounds, as well as in helimagnets in general, should belong to new universality classes with characteristic critical exponents that differ considerably from those for non-frustrated magnets with collinear spin structures. The order parameter of such systems includes, in addition to the ordinary spin variables, $\boldsymbol{S}_{\boldsymbol{R}}$, a new relevant variable, the chirality $\boldsymbol{K} = [\boldsymbol{S}_{\boldsymbol{R}_1} \times \boldsymbol{S}_{\boldsymbol{R}_2}]$, that describes whether the helically polarized spin structure is a right- or left-handed one. For example, due to the chiral degeneracy, the XY-antiferromagnet on a stacked triangular lattice does not have the symmetry of the order parameter V, namely S_1, as it does for the standard XY-model, but instead has the symmetry $Z_2 \times S_1$, where S_1 describes the symmetry of a unit vector in the XY-plane, and the two-element (Ising) group Z_2 describes the two possible directions of the normal to the XY-plane [2]. The corresponding critical exponents are $\alpha = 0.34(6)$, $\beta = 0.25(1)$, $\gamma = 1.13(5)$, $\nu = 0.54(2)$ [1, 3]. Recent Monte Carlo simulations [4] and numerous experimental data (see [5–7] and references therein) apparently confirm Kawamura's conjecture. Nevertheless, there is still considerable debate as regards this problem [8, 9]. For its complete examination one should study the average chirality, $\langle \boldsymbol{K} \rangle$, below T_N, and investigate its fluctuations above T_N. Unfortunately, the former will be accessible only in a single-domain crystal, while the latter are related to four-spin correlations, a direct experimental study of which is impossible.

0953-8984/98/050951+10$19.50

In reference [10] it was proposed that one might usefully study the projection of $\boldsymbol{K}$ on the sample magnetization induced by an applied magnetic field. This projection, which we call, following [10], the dynamical chirality (DC), determines the part of the purely inelastic cross section which is proportional to the neutron polarization $\boldsymbol{P}_0$. The polarization-dependent chiral contribution to the neutron scattering cross section was given as

$$\left(\frac{\mathrm{d}^2\sigma}{\mathrm{d}\Omega\ \mathrm{d}\omega}\right)_{P_0} = \frac{2}{\pi}\boldsymbol{P}_0(r_0\gamma F(\boldsymbol{Q}))^2\frac{k_f}{k_i}\frac{1}{1-\exp(-\omega/T)} \times (\hat{\boldsymbol{Q}}\cdot\hat{\boldsymbol{h}})^2\,\mathrm{Im}\,S_1(\boldsymbol{Q},\omega) + (\hat{\boldsymbol{h}}\cdot\hat{\boldsymbol{Q}})(\hat{\boldsymbol{Q}}\cdot\hat{\boldsymbol{c}})(\hat{\boldsymbol{c}}\cdot\hat{\boldsymbol{h}})\,\mathrm{Im}\,S_2(\boldsymbol{Q},\omega) \tag{1}$$

where $S_1 = 0$ for the XY-model and $S_2 = 0$ for the isotropic Heisenberg model, and the unit vectors are: $\hat{\boldsymbol{Q}}$, the scattering vector; $\hat{\boldsymbol{c}}$, along the axis perpendicular to the layers; and $\hat{\boldsymbol{h}}$, along the magnetic field direction. This expression was given in [10] without a derivation, together with that for small-angle scattering in ferromagnets [11], and it is worthwhile to give the derivation (we do this in the appendix of this paper). Here we only want to point out that the sign of the chiral cross section is not determined, and for $\omega \ll T$ it is an odd function of ω as was demonstrated experimentally in [12] for small-angle scattering in a ferromagnet. In a low magnetic field the chiral cross section should be proportional to the field. However, it is restricted by the condition that follows from the positiveness of the total differential cross section:

$$\left(\frac{\mathrm{d}^2\sigma}{\mathrm{d}\Omega\ \mathrm{d}\omega}\right)_0 > \frac{1}{P_0}\left|\left(\frac{\mathrm{d}^2\sigma}{\mathrm{d}\Omega\ \mathrm{d}\omega}\right)_{\boldsymbol{P}_0}\right| \tag{2}$$

where the left-hand side is the polarization-independent part of the cross section. Hence strong non-linearity should appear at higher fields.

In this paper we present the first results of a search for the effects of the dynamical chirality which was performed with a crystal of $CsMnBr_3$, an XY-antiferromagnet on a stacked triangular lattice. $CsMnBr_3$ has a hexagonal structure with space group $P6_3/mmc$ and lattice parameters $a = 7.61$ Å and $c = 6.52$ Å at room temperature [13]. The three-dimensional antiferromagnetic ordering of the Mn^{2+} spins, $S = 5/2$, occurs in zero field at $T_N = 8.37$ K [6]. The spins are restricted to a hexagonal plane, being ordered in the triangular structure [14] with a twofold-degenerate chiral ground state which is determined by clockwise or anticlockwise 120° spin rotation among the three nearest atoms of an in-plane triangle. The nearest neighbours in different planes are coupled antiferromagnetically with an exchange constant $J_0/k_B = -10.3$ K, which is much stronger than that, $J_1/k_B = -0.02$ K, in the plane [15]. As a result, $CsMnBr_3$ exhibits quasi-one-dimensional behaviour above about 15 K [16]. The application of a magnetic field in the [100] direction splits the antiferromagnetic transition, and the result is an intermediate phase with spin-flop character over a temperature range of about 0.1 K at $H = 10$ kOe [7].

A $CsMnBr_3$ single crystal of ellipsoidal shape with a volume of about 0.5 cm^3 was grown by the Bridgman technique from appropriate amounts of CsBr and $MnBr_2$. The crystal was oriented so as to have the $[1\bar{1}0]$ axis vertical (perpendicular to the scattering plane). The measurements were carried out at ILL, Grenoble, on the IN14 cold-neutron triple-axis spectrometer. The incident beam was monochromated by a pyrolytic graphite crystal and subsequently polarized by a supermirror bender. The sample was mounted in a fine-tail Orange cryostat at ILL inserted into the gap of a horizontal electromagnet providing fields up to 12 kOe along the direction of the scattering vector $\hat{\boldsymbol{Q}}$. The beam polarization in this set-up, as determined with a Heusler analyser, was about 90% (a flipping ratio of 20). First of all, to obtain the intensity we measured the chiral cross section (1) integrated

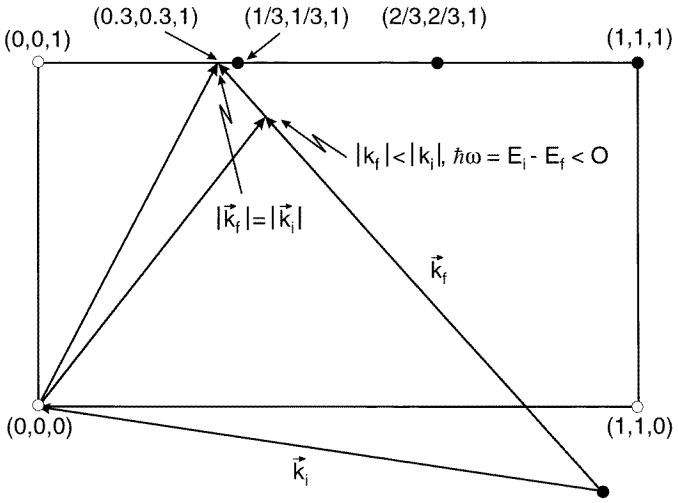

Figure 1. The plane investigated, in reciprocal space. The magnetic points are shown by closed circles. The diagrams for the elastic scattering at the $(0.3, 0.3, 1)$ point and the integration of the energy over the neutron energy loss (along $\boldsymbol{k}_f$) are shown.

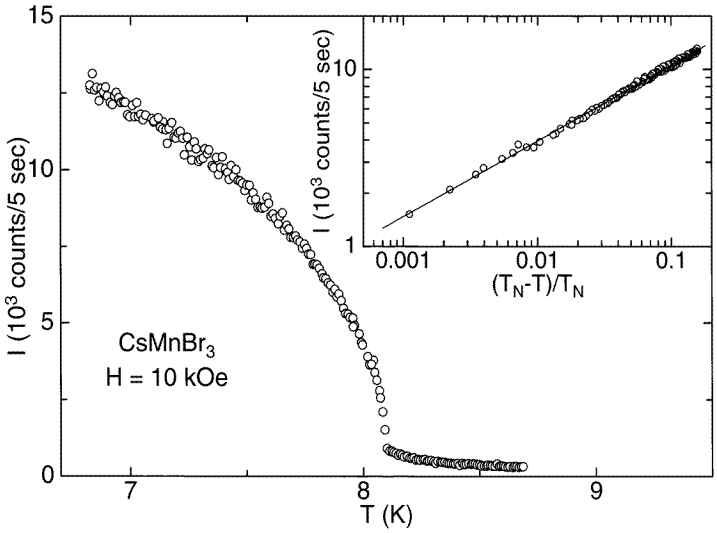

Figure 2. The temperature dependence of the magnetic Bragg intensity, I, at $(1/3, 1/3, 1)$ in $H = 10$ kOe. A log–log plot of the magnetic intensity versus the reduced temperature, $\tau = (T_N - T)/T_N$, is shown in the inset. The straight line is a fit of the form $I \sim |\tau|^{2\beta}$ with $\beta = 0.22(1)$.

over the energy transfer, ω. As it is an odd function of ω, such an integration should give zero. However, we have used a technique that allows us to integrate just over the neutron energy losses ($\omega = E_f - E_i < 0$) where E_f and E_i are the energies of the scattered and incident neutrons respectively. For this purpose the measurements were carried out with a Be filter replacing the analyser. The energy of the incident neutrons was chosen to lie in the

middle of the filter transmission edge—$E_i = 5.24$ meV ($k_i = 1.59$ Å^{-1})—so that most of the detected intensity would correspond to energy-loss scattering. The scattering diagram is shown in figure 1, where the magnetic reciprocal-lattice points are shown as closed circles.

To find the experimental values of the Néel point in applied magnetic fields, the temperature dependence of the intensity I at the magnetic reflection point $(1/3, 1/3, 1)$ has been measured in 2.5 kOe and in 10 kOe (figure 2). Sharp transitions at 8.09 K in 2.5 kOe and at 8.10 K in 10 kOe have been found. The difference of 0.28 K from T_N obtained at $H = 0$ in [6] can be attributed to the large distance between the thermometer and the sample in the actual experimental set-up. The critical exponent β which corresponds to the order parameter was obtained from these measurements by means of a log–log plot as shown in the inset of figure 2. The extracted value, $\beta = 0.22(1)$ at $H = 10$ kOe, agrees with the theoretical prediction of 0.25(1) for the $Z_2 \times S_1$ universality class [3] as well as with the previously determined experimental values $\beta = 0.25(1)$ [17] and $\beta = 0.21(2)$ [18].

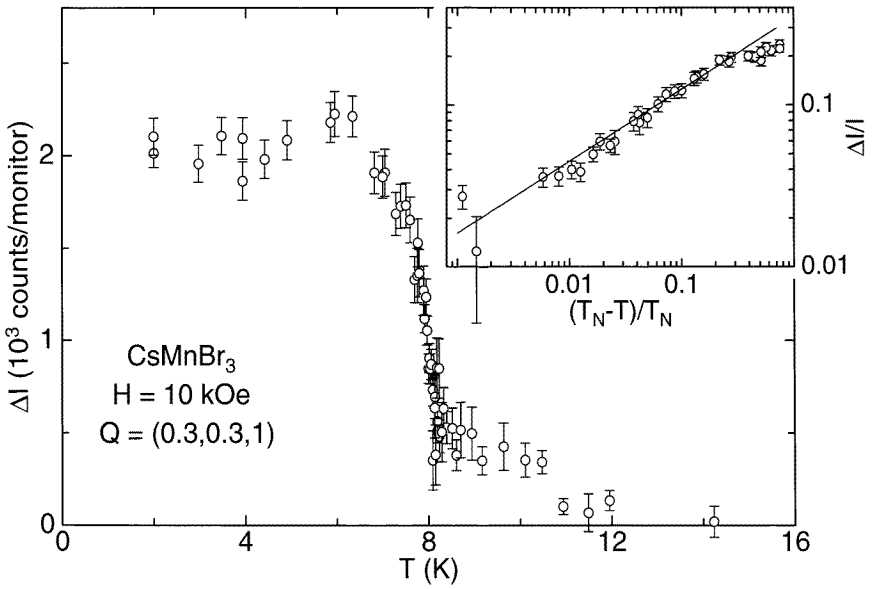

Figure 3. The temperature dependence of $\Delta I = I^{on} - I^{off}$ integrated over the neutron energy loss at $H = 10$ kOe. A log–log plot of the ratio $\Delta I/I$, where $I = I^{on} + I^{off}$, versus the reduced temperature is shown in the inset. The straight line is the best fit with the critical exponent 0.44(6).

The chiral cross section (1) integrated over $0 > \omega > -E_i$ is proportional to the intensity difference, $\Delta I = I^{on} - I^{off}$, between the two values measured with a Be filter for opposite neutron polarizations, i.e., with the spin flipper switched on, I^{on}, and off, I^{off}. The temperature dependence of ΔI at the reciprocal-lattice point $(0.3, 0.3, 1)$ is shown in figure 3. It is very flat, having the dependence $\tau^{-0.18(10)}$ ($\tau = (T - T_N)/T_N$) over the temperature range 8.19 K $\leqslant T \leqslant$ 11.95 K ($0.011 \leqslant \tau \leqslant 0.495$). A prediction for this exponent, $\varphi_K + \gamma = 2.33(11)$, has been made in [10], but one has to keep in mind that this is valid only for $\boldsymbol{q} = \boldsymbol{Q} - \boldsymbol{Q}(1/3, 1/3, 1) = 0$. At the same time, if q is much higher than the inverse correlation length, κ, the divergence can be shown to be much weaker (as $\tau^{-0.4}$). According to the inverse-correlation-length data [18], our measurements were done with $q > \kappa$ at the lowest τ and $q < \kappa$ at the highest τ. In this situation it is

impossible to give any simple prediction for the temperature dependence of ΔI. However, taking into account that the resolution ellipsoid widths (FWHM), $\Delta Q_x = 0.014$ Å^{-1}, $\Delta Q_y = 0.026$ Å^{-1}, are comparable with q and κ, as well as the fact that the values of $\boldsymbol{q}$ corresponding to inelastic processes can even be higher than that of the 'elastic' momentum $\boldsymbol{q} = \boldsymbol{Q}(0.3, 0.3, 1) - \boldsymbol{Q}(1/3, 1/3, 1)$, the temperature dependence of ΔI found in this experiment above T_N seems to be reasonable.

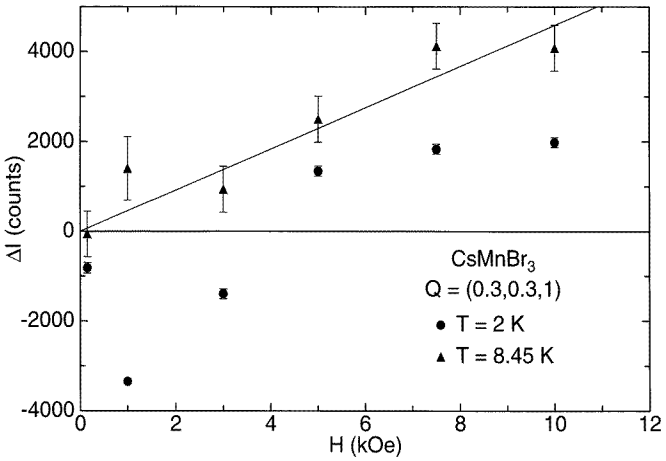

Figure 4. The field dependence of $\Delta I = I^{on} - I^{off}$ integrated over the neutron energy loss at $T = 2$ K (with ΔI measured in counts/5 min) and at $T = 8.45$ K (with ΔI measured in counts/39 min).

From figure 4 it is seen that ΔI above the Néel point ($T = 8.45$ K) is proportional to the external field, as it should be for the chiral cross section [10] in the approximation of small field. In our case this approximation is valid at least up to $H = 10$ kOe.

The most striking feature of the integrated intensity data is a strong increase of the DC scattering below T_N (figure 3), and its non-monotonic behaviour as a function of magnetic field at $T = 2$ K (figure 4). It was shown in references [10, 11] (see also the appendix) that the DC scattering is entirely inelastic. Thus, below T_N it should be attributed to the low-energy magnetic excitations. According to [10], in the case of a conventional two-sublattice antiferromagnet in a magnetic field $\boldsymbol{H}$ perpendicular to the sublattice magnetization, the function $\mathrm{Im}\, S_1$ in equation (2) is given by

$$\mathrm{Im}\, S_1 = \frac{2g\mu H S^2 J_0 T}{\epsilon_q^2 + (g\mu H)^2}[\delta(\omega - \epsilon_q) - \delta(\omega + \epsilon_q)]P_0 \tag{3}$$

where $J_0 = \sum J_R$, and ϵ_q is the spin-wave energy. The corresponding contribution of the DC scattering intensity integrated over $\omega < 0$ is proportional to

$$\Delta I \sim -\frac{2g\mu H S^2 J_0 T P_0}{\epsilon_q[\epsilon_q^2 + (g\mu H)^2]}. \tag{4}$$

Here, the right-hand side is a linear function of the magnetic field, H, if $g\mu H$ is much less than the spin-wave energy, ϵ_q. It has a maximum at $g\mu H = \epsilon_q$ and decreases for $g\mu H \gg \epsilon_q$. Qualitatively, such behaviour should occur for any well defined or diffusive-like magnetic excitations with characteristic energy ϵ_q. However, the sign of the extremum cannot be predicted in the general case.

Let us consider now the field dependence of ΔI at $T = 2$ K shown in figure 4. One can see a deep minimum at a value of H between 1 and 2 kOe that is followed by a smooth increase of ΔI up to the maximal value at $H \approx 10$ kOe. The gradual increase of ΔI with H is apparently attributable to the acoustic spin wave observed in $CsMnBr_3$ [19]. According to these data, the spin waves have an interplane dispersion in the form

$$\epsilon_q \approx (Q - 1/3, Q - 1/3, 0) \times 4.3 \text{ meV}. \tag{5}$$

In our case $q = Q - 1/3 = 0.03$, and $\epsilon_q = 0.13$ meV. This corresponds to a field $H = 11$ kOe for $g = 2$. As $\boldsymbol{H}$ is along $\boldsymbol{Q} = (1/3, 1/3, 1)$, the $\hat{c}$-component of $\boldsymbol{H}$ is equal to 9.4 kOe. Thus, at $H = 10$ kOe we are near the maximal value of the DC cross section related to the acoustic spin waves. At the same time the minimum of ΔI seen in figure 4 should be attributed to a new low-energy mode with $\epsilon_q \approx 0.02$ meV at $q = 0.03$. Because of its very low energy, this mode cannot be observed in a conventional inelastic neutron scattering experiment like that described in [19]. Apparently this mode is connected with the $Z_2 \times S_1$ symmetry of the system. In this case we may consider it as a new type of topological excitation. We are planning to continue our DC scattering studies in order to determine the dispersion of this mode.

The temperature dependence of the ratio $\Delta I/I$, where $I = I^{\text{on}} + I^{\text{off}}$, below T_N at $H = 10$ kOe, shown as a log–log plot in the inset of figure 3, should mainly be attributed to a renormalization of the spin-wave spectrum in the critical region near T_N. Indeed, the polarization-independent spin-wave scattering intensity at $\omega < 0$ is given by

$$I = S^2 J_0 T/\epsilon_q^2 \tag{6}$$

and we get

$$\frac{\Delta I}{I} = \frac{\epsilon_q g\mu H}{\epsilon_q^2 + (g\mu H)^2} \approx \frac{\epsilon_q}{g\mu H}. \tag{7}$$

The right-hand side of this expression has to be independent of the detailed form of the spin-wave excitations.

According to the dynamical scaling, we may write ϵ_q as a function of the reduced temperature, $\tau = (T - T_N)/T_N$, in the following form:

$$\epsilon_q = \epsilon_c |\tau|^{\nu(z-1)} (Q - 1/3, Q - 1/3, 0) \tag{8}$$

where ν is the correlation length exponent and z is the dynamical critical exponent. The former has been determined for $CsMnBr_3$ experimentally [18] as $\nu = 0.54(3)$, in good agreement with the theoretical value, $\nu = 0.53(2)$ [1]. The dynamical exponent, z, has been measured in reference [20] for $q < 0.07$, and is equal to 1.47(6). As a result, for the exponent in equation (8) we get $\nu(z - 1) = 0.25(4)$. Experimentally, we found for this exponent a value of 0.44(6), as shown by the straight line in the inset of figure 3. The difference is only 2.6 standard deviations, and we might get an even better agreement if we were to take the new low-energy excitation into account.

The differential chiral cross section (1) has been investigated at $T = 8.45$ K in $H = 10$ kOe using a pyrolytic graphite crystal as the energy analyser. The difference $\Delta I_\omega = I_\omega^{\text{on}} - I_\omega^{\text{off}}$ at a given energy transfer, ω, which is proportional to

$$\left(\frac{\mathrm{d}^2\sigma}{\mathrm{d}\Omega\ \mathrm{d}\omega}\right)_{\boldsymbol{P}_0}$$

is shown in figure 5, by closed circles, together with the sum $I_\omega = I_\omega^{\text{on}} + I_\omega^{\text{off}}$ (open circles), which is proportional to the polarization-independent differential cross section of

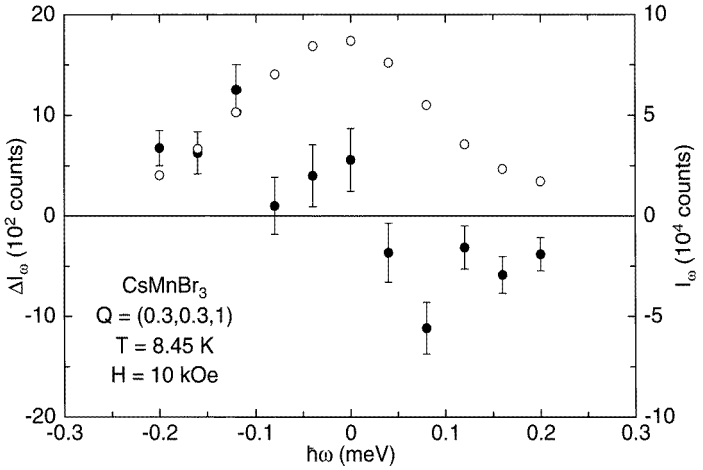

Figure 5. The neutron scattering intensities $\Delta I_\omega = I_\omega^{\rm on} - I_\omega^{\rm off}$ (closed circles, left-hand scale) and $I_\omega = I_\omega^{\rm on} + I_\omega^{\rm off}$ (open circles, right-hand scale) at a fixed neutron energy transfer, ω, as functions of ω ($T = 8.45$ K and $H = 10$ kOe).

the magnetic scattering

$$\left(\frac{{\rm d}^2\sigma}{{\rm d}\Omega\ {\rm d}\omega}\right)_0.$$

In spite of the rather large error bars obtained in this experiment, it is evident that the differential chiral cross section is antisymmetric in energy transfer. $|\Delta I_\omega|$ for the maxima at $\omega = \pm 0.12$ meV is about a tenth of I_ω, i.e., we are still far from the limit given by (2).

In conclusion, we have observed for the first time the effects of the dynamical chirality in the TLA $CsMnBr_3$ above and below the Néel point. In the paramagnetic phase near $T_{\rm N}$, we have demonstrated the antisymmetry in the energy transfer of the spin-dependent part of the magnetic cross section and its linear dependence on magnetic field. In the ordered phase near $T_{\rm N}$, a qualitative agreement of the spin-wave contribution to the DC scattering with the predictions of the dynamical scaling has been found. A new low-energy excitation has been observed at $T = 2$ K which is presumably of topological origin. The study of the dispersion of this excitation by means of field-dependent measurements like those for which the results are displayed in figure 4 but at different $\boldsymbol{Q}$ should clear up the last point.

Acknowledgments

We are grateful to the ILL for hospitality. This work was partly supported by the Russian Federal Foundation for Neutron Studies on Condensed Matter and by the grants 96-02-18037a and 96-02-18673 from the Russian Foundation for Fundamental Research and the Russian Programme on Statistical Physics.

Appendix

In this appendix we present a derivation of the DC contribution (1) to the neutron scattering cross section. This contribution was given previously without derivation. Some of the

features have been formulated for small-angle scattering in ferromagnets [11] and for the general case [10].

We begin with the well known expression for the magnetic scattering amplitude which can be represented in two equivalent forms:

$$f_{mn}(\boldsymbol{Q}) = -r_0\gamma F(\boldsymbol{Q})\boldsymbol{S}_{\boldsymbol{Q}mn\perp}\cdot\boldsymbol{\sigma} = -r_0\gamma F(\boldsymbol{Q})\boldsymbol{S}_{\boldsymbol{Q}mn}\cdot\boldsymbol{\sigma}_\perp \tag{A1}$$

where n and m label the initial and final states of the scatterer, with the energies E_n and E_m. The first form is the conventional one. However, if one needs to analyse the symmetry of the susceptibility tensor $\chi_{\alpha\beta}$, it is more convenient to use the second representation. The corresponding expression for the cross section is

$$\frac{\mathrm{d}\sigma}{\mathrm{d}\Omega} = (r_0\gamma F(\boldsymbol{Q}))^2\frac{k_f}{k_i}\sum_{nm}\frac{\exp(-E_n/T)}{Z}S^\beta_{-\boldsymbol{Q}nm}S^\alpha_{\boldsymbol{Q}mn}\delta(\omega+E_{mn})\overline{\boldsymbol{\sigma}^\beta_\perp\boldsymbol{\sigma}^\alpha_\perp} \tag{A2}$$

where $\omega = E_f - E_i$, $E_{mn} = E_m - E_n$, $Z = \sum_n \exp(-E_n/T)$, and the bar indicates averaging over the spin states of the neutron beam. Making use of $\boldsymbol{\sigma}^\alpha\boldsymbol{\sigma}^\beta = \delta_{\alpha\beta} + \mathrm{i}\varepsilon_{\alpha\beta\gamma}$, we obtain

$$\overline{\boldsymbol{\sigma}^\beta_\perp\boldsymbol{\sigma}^\alpha_\perp} = (\delta_{\alpha\beta} - \hat{Q}_\alpha\hat{Q}_\beta) + \mathrm{i}(\epsilon_{\beta\alpha\gamma} + \hat{Q}_\beta\hat{Q}_\mu\epsilon_{\alpha\mu\gamma} - \hat{Q}_\alpha\hat{Q}_\mu\epsilon_{\beta\mu\gamma})P_{0\gamma} \tag{A3}$$

where $\epsilon_{\beta\alpha\gamma}$ is the antisymmetric unit pseudotensor. The expression in the first bracket is a symmetric tensor that is generally used for conventional derivation of the cross section. The second term is antisymmetric under permutation of the indices α and β and is proportional to the neutron polarization $\boldsymbol{P}_0$.

As we shall see below, in the cross-section expression this part is multiplied by the antisymmetric part of the generalized susceptibility. This susceptibility is determined in the usual way:

$$\chi_{\beta\alpha}(\boldsymbol{Q},\omega) = \mathrm{i}\int_0^\infty \mathrm{d}t\ \mathrm{e}^{\mathrm{i}\omega t}\left\langle[S^\beta_{-Q}(t), S^\alpha_Q(0)]\right\rangle \tag{A4}$$

where $[A, B] = AB - BA$, and $\langle\cdots\rangle$ is the Gibbs average which is determined as $\sum_n Z^{-1}\exp(-E_n/T)$.

From time-reversal symmetry (expression (127.14) from reference [21]) we have

$$\chi_{\beta\alpha}(\boldsymbol{H}) = \chi_{\alpha\beta}(-\boldsymbol{H}) \tag{A5}$$

where $\boldsymbol{H}$ is the magnetic field or spontaneous magnetization. In particular, the tensor $\chi_{\beta\alpha}$ is symmetric if $\boldsymbol{H} = 0$. For $\boldsymbol{H} \neq 0$ the susceptibility may be divided into symmetric (S) and antisymmetric (A) parts:

$$\chi^{(\mathrm{S})}_{\beta\alpha} = \frac{1}{2}(\chi_{\beta\alpha} + \chi_{\alpha\beta}) \qquad \chi^{(\mathrm{A})}_{\beta\alpha} = \frac{1}{2}(\chi_{\beta\alpha} - \chi_{\alpha\beta}). \tag{A6}$$

The spectral representation for the susceptibility is given by the well known expression

$$\chi_{\beta\alpha}(\omega) = -\sum_{nm}\frac{\exp(-E_n/T)}{Z}\frac{S^\beta_{nm}S^\alpha_{mn}[1-\exp(-E_{mn}/T)]}{E_{mn}+\omega+\mathrm{i}\delta} \tag{A7}$$

which can be easily derived by the method given in reference [21], chapter 127. Using conventional decomposition,

$$(E_{mn}+\omega+\mathrm{i}\delta)^{-1} = \mathrm{P}(E_{mn}+\omega)^{-1} - \mathrm{i}\pi\delta/(E_{mn}+\omega) \tag{A8}$$

where 'P' denotes the principal part, we select from $\chi_{\beta\alpha}$ the δ-function contribution that determines the cross section. It should be noted however that this contribution does not

coincide with Im $\chi_{\beta\alpha}$. The corresponding symmetric and antisymmetric parts of $\delta\chi_{\beta\alpha}$ may be written as follows:

$$\delta\chi_{\beta\alpha}^{(\mathrm{S,A})} = \mathrm{i}\pi \sum_{nm} \frac{\exp(-E_n/T)}{Z}(S_{nm}^{\beta}S_{mn}^{\alpha} \pm S_{nm}^{\alpha}S_{mn}^{\beta})\delta(\omega + E_{mn})(1 - \mathrm{e}^{-\omega/T}). \tag{A9}$$

By use of the hermiticity, $S_{nm}^{*} = S_{mn}$, one obtains that $\delta\chi_{\beta\alpha}^{(\mathrm{S})}$ is imaginary and $\delta\chi_{\beta\alpha}^{(\mathrm{A})}$ is real. As a result, the polarization-independent part of the cross section may be represented in the usual way:

$$\left(\frac{\mathrm{d}^2\sigma}{\mathrm{d}\Omega\ \mathrm{d}\omega}\right)_0 = (r_0\gamma F(\boldsymbol{Q}))^2\frac{k_f}{k_i}\frac{\mathrm{Im}\,\chi_{\beta\alpha}^{(\mathrm{S})}(\boldsymbol{Q},\omega)}{\pi(1-\mathrm{e}^{-\omega/T})}(\delta_{\beta\alpha} - \hat{Q}_\beta\hat{Q}_\alpha). \tag{A10}$$

It is convenient to determine a function $S_{\beta\alpha}(\omega) = \mathrm{i}\chi_{\beta\alpha}^{(\mathrm{A})}$. The polarization-dependent chiral part of the cross section is given by the general expression

$$\left(\frac{\mathrm{d}^2\sigma}{\mathrm{d}\Omega\ \mathrm{d}\omega}\right)_{\boldsymbol{P}_0} = (r_0\gamma F(\boldsymbol{Q}))^2\frac{k_f}{k_i}\frac{\mathrm{Im}\,S_{\beta\alpha}(\omega)}{\pi(1-\mathrm{e}^{-\omega/T})}(\epsilon_{\beta\alpha\gamma} + \hat{Q}_\beta\hat{Q}_\mu\epsilon_{\alpha\mu\gamma} - \hat{Q}_\alpha\hat{Q}_\mu\epsilon_{\beta\mu\gamma})P_{0\gamma}. \tag{A11}$$

Let us consider now some properties of $S_{\beta\alpha}(\omega)$. From equations (A8) and (A9) we immediately conclude that Im $S_{\beta\alpha}$ and Re$S_{\beta\alpha}$ are even and odd functions of ω, respectively, and Im $S(0) = 0$ as it should. For the isotropic case (the Heisenberg model)

$$S_{\beta\alpha} = \epsilon_{\beta\alpha\rho}\hat{\boldsymbol{m}}_\rho S_H(\omega) \tag{A12}$$

where $\hat{\boldsymbol{m}}$ is a unit vector along the sample magnetization direction, we have

$$\left(\frac{\mathrm{d}^2\sigma}{\mathrm{d}\Omega\ \mathrm{d}\omega}\right)_{\boldsymbol{P}_0} = 2(r_0\gamma F(\boldsymbol{Q}))^2\frac{k_f}{k_i}\frac{\mathrm{Im}\,S_H(\boldsymbol{Q},\omega)}{\pi(1-\mathrm{e}^{-\omega/T})}(\hat{\boldsymbol{Q}}\cdot\hat{\boldsymbol{m}})(\hat{\boldsymbol{Q}}\cdot\hat{\boldsymbol{P}}_0). \tag{A13}$$

For planar magnets (the XY-model), the antisymmetric part of $\chi_{\beta\alpha}$ appears as a vector product of neighbouring spins that is directed perpendicularly to the plane (along the $\hat{\boldsymbol{c}}$-axis). As a result we have [10]

$$S_{\beta\alpha} = \epsilon_{\beta\alpha\rho}\hat{c}_\rho(\hat{\boldsymbol{c}}\cdot\hat{\boldsymbol{m}})S_{XY}(\omega) \tag{A14}$$

and

$$\left(\frac{\mathrm{d}^2\sigma}{\mathrm{d}\Omega\ \mathrm{d}\omega}\right)_{\boldsymbol{P}_0} = 2(r_0\gamma F(\boldsymbol{Q}))^2\frac{k_f}{k_i}\frac{\mathrm{Im}\,S_{XY}(\boldsymbol{Q},\omega)}{\pi(1-\mathrm{e}^{-\omega/T})}(\hat{\boldsymbol{c}}\cdot\hat{\boldsymbol{Q}})(\hat{\boldsymbol{Q}}\cdot\hat{\boldsymbol{P}}_0)(\hat{\boldsymbol{c}}\cdot\hat{\boldsymbol{m}}). \tag{A15}$$

In the general case of uniaxial crystals, the chiral cross section is the sum of equations (A13) and (A15). If we take into account that, as a rule, neutrons are polarized along the direction of the field or in the opposite direction, we arrive at the chiral cross section (1).

References

[1] Kawamura H 1992 *J. Phys. Soc. Japan* **61** 1299
[2] Kawamura H and Miyashita S 1984 *J. Phys. Soc. Japan* **53** 4138
[3] Kawamura H 1988 *J. Appl. Phys.* **63** 3086
[4] Dobry A and Diep H T 1995 *Phys. Rev.* B **51** 6731
[5] Wang J, Belanger D P and Gaulin B D 1991 *Phys. Rev. Lett.* **66** 3195
[6] Deutschmann R, von Löhneysen H, Wosnitza J, Kremer R K and Visser D 1992 *Europhys. Lett.* **17** 637
[7] Weber H, Beckmann D, Wosnitza J, von Löhneysen H and Visser D 1995 *Int. J. Mod. Phys.* B **9** 1387
[8] Azaria P, Delamotte B and Jolicoeur T 1990 *Phys. Rev. Lett.* **64** 3175
[9] Antonenko S A and Sokolov A I 1994 *Phys. Rev.* B **49** 1590
[10] Maleyev S V 1995 *Phys. Rev. Lett.* **75** 4682

[11] Lazuta A V, Maleyev S V and Toperverg B P 1981 *Zh. Eksp. Teor. Fiz.* **81** 1475 (Engl. Transl. 1981 *Sov. Phys.–JETP* **54** 782)
[12] Okorokov A I, Gukasov A G, Slyusar V N, Toperverg B P, Scharpf O and Fujara F 1983 *Pis. Zh. Eksp. Teor. Fiz.* **37** 269 (Engl. Transl. 1983 *JETP Lett.* **37** 319)
[13] Goodyear G and Kennedy D J 1974 *Acta Crystallogr.* B **28** 1640
[14] Eibshütz M, Sherwood R C, Hsu F C L and Cox D E 1974 *Thermal Expansion 1973 (AIP Conf. Proc. No 10)* ed R E Taylor and G L Denman (New York: American Institute of Physics Publishing) p 684
[15] Breitling W, Lehmann W, Weber R and Wagner W 1977 *J. Magn. Magn. Mater.* **6** 113
Collins M F and Gaulin B D 1984 *J. Appl. Phys.* **55** 1869
Gaulin B D, Collins M F and Buyers W J L 1987 *J. Appl. Phys.* **61** 3409
[16] Gaulin B D and Collins M F 1984 *Can. J. Phys.* **62** 1132
[17] Ajiro Y, Nakashima T, Unno Y, Kadowaki H, Mekata M and Achiwa N 1988 *J. Phys. Soc. Japan* **57** 2648
[18] Mason T E, Gaulin B D and Collins M F 1989 *Phys. Rev.* B **39** 586
[19] Inami T, Kakurai K, Tanaka H, Enderle M and Steiner M 1995 *Physica* B **213–214** 167
[20] Mason T E, Yang Y S, Collins M F, Gaulin B D and Clausen K N 1992 *J. Magn. Magn. Mater.* **104–107** 197
[21] Landau L D and Lifshitz E M 1976 *Statisticheskaya Fizika* part 1, 3rd Russian edn (Moskva: Nauka) (Engl. Transl. 1968 *Statistical Physics* (Oxford: Pergamon))